Exploration Geophysics (1996) ***27****, 77-89*

Three component DHEM surveying at Balcooma

N.A. Hughes
Pasminco Exploration
380 St Kilda Road, Melbourne,
Victoria, Australia

William R. Ravenhurst
Crone Geophysics & Exploration Ltd
3607 Wolfedale Road, Mississauga,
Ontario, Canada

SUMMARY

A comparative survey using multi-loop axial DHEM and three component DHEM was undertaken on the Balcooma deposit, North Queensland by Crone Geophysics & Exploration Ltd., in 1991. Unlike the axial data, results from the three component data are unambiguous as to the location and orientation of a previously undetected extension of a mineralized lens.

The paper shows how cross-component data can be corrected for probe rotation down the hole using the primary field and suggests that vector presentation of results can aid interpretation.

Keywords: Drillhole EM, Primary Pulse, axial, three components, multiple loops, filament, vectors, Balcooma

INTRODUCTION

In axial component drill hole electromagnetic (DHEM) surveys of isolated drill-holes it is customary to use multiple transmitter loops to:

- ensure all potential conductors are energized,
- determine the azimuth location or quadrant in which the conductor lies, and
- ensure positional discrimination of multiple close-spaced conductors.

Measuring the three components of the secondary magnetic field may allow the use of fewer transmitter loops and usually leads to more confidence in the interpretation of azimuth, orientation and size of the conductor, including conductors intersected by the borehole.

HISTORY

In January 1991 Crone Geophysics developed a three component DHEM system in co-operation with Noranda Exploration Co. Ltd. (Hodges and Crone, 1991) with the specific aim of better resolving closely spaced conductors fro the borehole. The system was successfully trailed at Noranda's Heath Steele deposit in New Brunswick, Canada. In November 1991 the system was used at the Balcooma deposit in North Queensland for Lachlan Resources and this is believed to be the first commercial application of three component DHEM surveying in Australia.

SURVEY PROCEDURE AND EQUIPMENT DESIGN

The Crone three component DHEM system uses two probes. One measures the component parallel to the drill hole trajectory, called the axial probe, the other, called the XY, or cross component probe, measures the two orthogonal axes. Thus the hole is logged twice to obtain all three components. Although this procedure can be time consuming, the results from the axial probe survey often dictates whether or not cross-component data are required.

The XY probe was designed to be compatible with other Crone EM equipment and uses the same two conductor cable and attachment head as the axial probe. As a result only one component of the cross axis data can be recorded at a time. Component selection was originally controlled through a switching device attached to the borehole slip-ring, but is now controlled by software in the receiver.

System Measurements

The Crone EM system operates in the time domain and measures both the decay of the secondary magnetic field, over a number of semi logarithmic time windows, as well as a single channel within the shut-off ramp (Figure 1). This ramp is controlled and has a width of 0.5, 1.0, or 1.5 milliseconds. Measurement times are referenced from the end of the ramp. The value recorded in the ramp, termed the Primary Pulse (PP), is nominally from –199 microseconds to –99 microseconds.

There are several present time window channel files, but users have the option of defining their own windows. The latest equipment also has an uncontrolled (fast) ramp, as well as the three controlled linear ramps.

Definition of Coordinates

Crone define a local XYZ coordinate system to present their data, where Z is the axial direction, positive towards the hole collar; X is orthogonal to Z, in the vertical plane and positive up (and parallels the local azimuth of the hole); and Y is orthogonal to the XY plane, with its direction producing a right handed coordinate system (Figure 2). (The letters X, Y, Z are now more commonly used to describe fixed coordinates, with U, V, A (respectively) reserved for local axes.

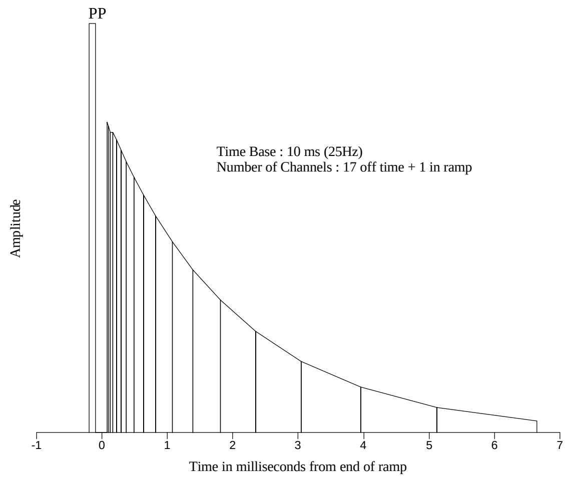

Figure 1. Position of time-decay windows for Crone Pulse EM System 20 channel window option (including PP channel). For a 10msec off time only the first 17 channels are recorded.

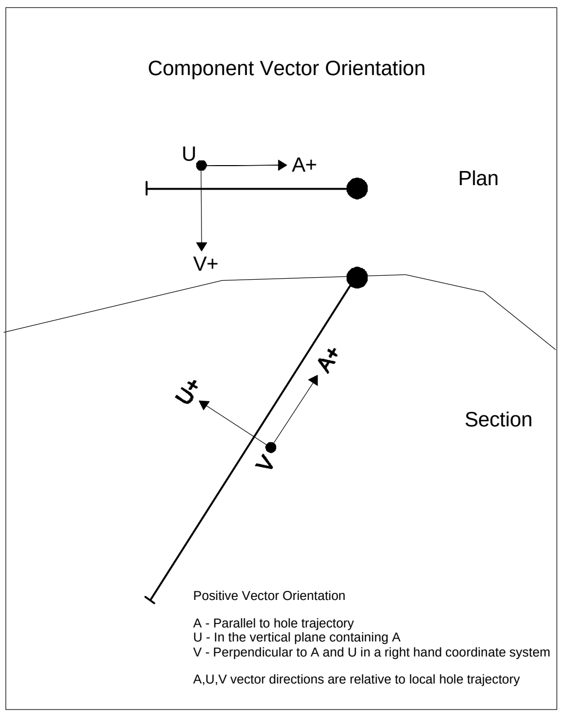

Figure 2. Definition of coordinate system for multi-component data. 'U' and 'V' are local axes which move in sympathy with the drill-hole azimuth.

Correction for XY Probe Rotation

Probes have a tendency to rotate as they are moved up and down a drill-hole (although experience has show that except in steep holes this is generally a rare and sudden event) and orientations of the cross-component coils need to be determined to correct for this rotation. Prior to the introduction of a dip and rotation tool, this correction was effected by comparing the measured and calculated Primary Pulse (PP) for X and Y. This method, called the Primary Pulse method is still often used as a check.

The PP method requires a good knowledge of the loop layout as well as accurate hole deviation data. Where possible, transmitter loop design should be such as to make it obvious what the X and Y PP polarities should be. Difficulties in accurately resolving the amount of probe rotation can arise if the loop is placed so as to have little or no PP amplitude in the X-Y plane. This problem has been solved by using a small locater loop which gives unambiguous PP field directions. PP readings are made from both loops for every station down the hole.

In areas of conductive cover or host, or close to a good conductor, the PP measured in the drill hole will be distorted and not generally correlate to that calculated for free space. To compensate, a routine was devised whereby the distortion to the PP is calculated from the measured secondary field. Referred to as "Primary Pulse Cleaning", this system works well in areas of low noise and where the secondary field has decayed to zero. This technique is described in the APPENDIX.

A more recent XY probe developed by Crone (1993) has an additional attachment (called the "Orientation Tool") used for measuring dip and rotation. This works well for holes with dips between 20° and 87° from horizontal, but as previously stated the PP method is still useful for checking the rotation correction.

CASE HISTORY: DHEM SURVEYING AT BALCOOMA

The advantage of three component over one component data is illustrated using results from a survey over the Balcooma deposit in north Queensland. The results are also used to show examples of the rotation technique described in the appendix.

Geology

The Balcooma volcanogenic massive sulphides (VMS) deposit was discovered in 1974 by CEC investigating a lead-rich gossan (Harvey, 1984). It has an estimated resource of 3.5 Mt at 3.0% Cu with significant amounts of Pb+Zn and is the largest of eight separate deposits which together make up the Dry River Group (Figure 3), with a total resource of ~6 Mt of copper rich polymetallic mineralisation (Huston, 1990).

The deposits are hosted by the lower amphibolite facies Balcooma Metamorphics, a 40 km long northeast-trending belt bounded dominantly by undeformed granitic rocks and in the northeast by the Oaky Creek mylonite zone. The belt comprises three main rock types; metamorphosed interbedded greywacke and pelite, quartz-muscovite-biotite schist, and quartz-feldspar porphyry, and has a complex deformational history with at least four cleavage-forming events (Huston, 1990).

There are four separate ore lenses at Balcooma (referred to as Zones 1 to 4), which are hosted in different lithostratigraphic horizons. Three of the lenses contain Zn-Pb-Ag-(Cu-Au), whereas the other contains Cu-(Ag-Au). There are three distinct ore assemblages:

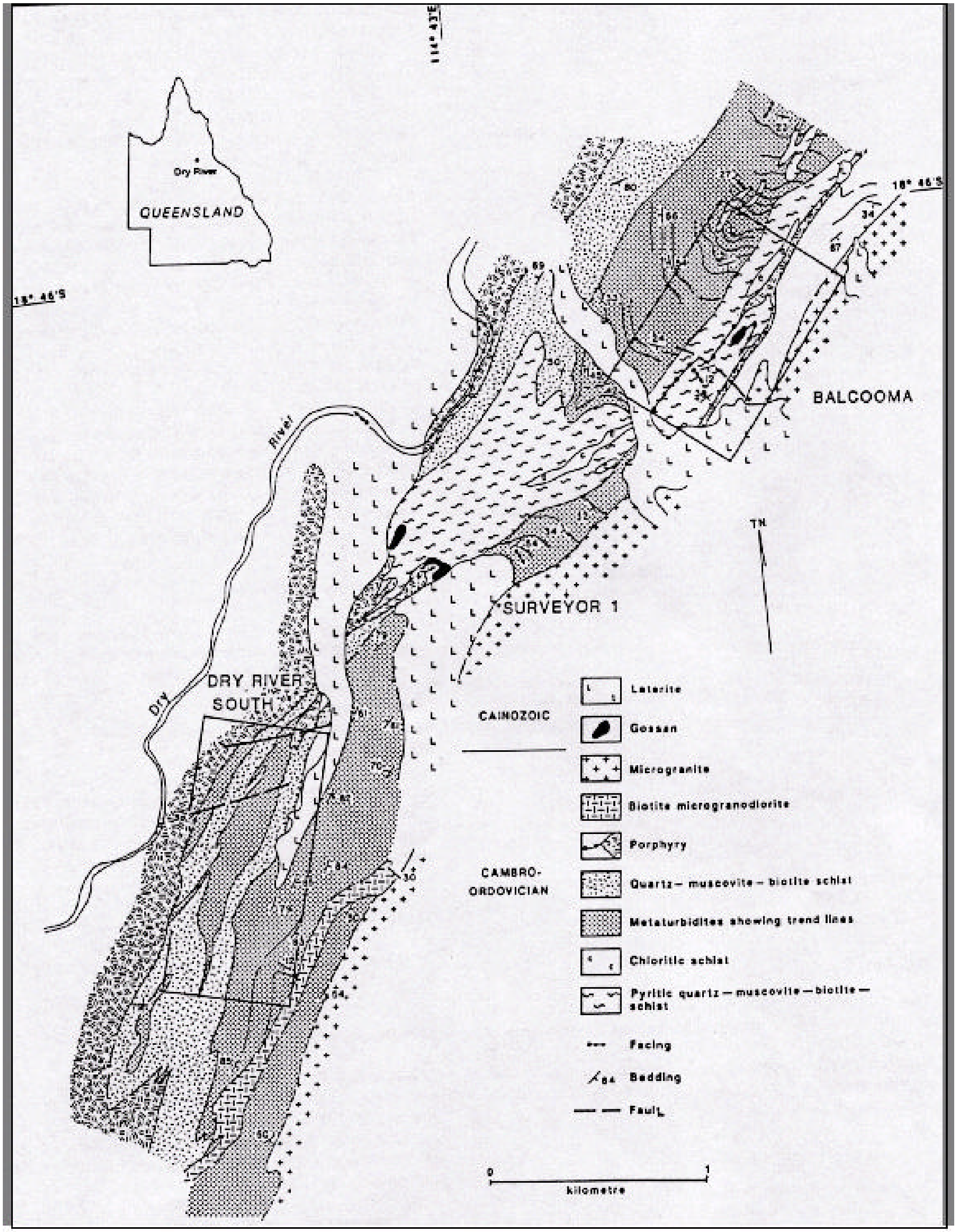

Figure 3. Location of Balcooma deposit & regional geology (after Huston, 1990).

- Massive magnetite with accessory pyrite, chalcopyrite, pyrrhotite and chlorite,
- Massive pyrite-chalcopyrite with minor pyrite and magnetite, and
- Massive sphalerite-galena-pyrite minor chalcopyrite, arsenopyrite and tetrahedrite.

In long section (Figure 4) the ore lenses are elongate sub-parallel to the general fabric of the country-rock, and trend to the north-east, whereas in cross-sectional view the lenses are confined ellipses which dip south-east (Figure 5). Therefore, the lenses are elliptical shoots which plunge moderately south, 15° to 25°, within the main structural fabric (Huston, 1990).

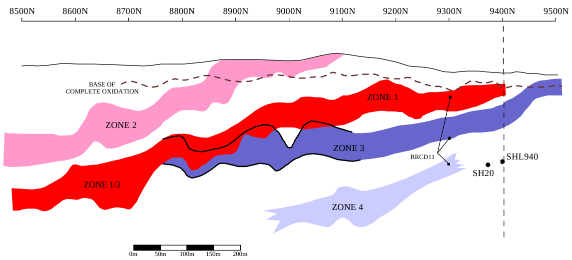

Figure 4. Long section showing mineralised zones and drill-holes discussed in this paper (modified after Plutonic Annual Report, 1992).

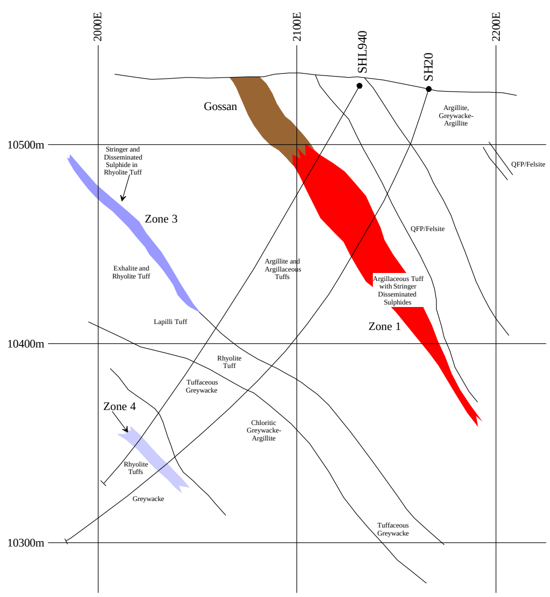

Figure 5. Geological cross section at 9400N showing the location of SHL940 and SH20.

DHEM surveying

Lachlan Resources contracted Crone Geophysics & Exploration Limited to undertake DHEM surveys to test for extensions to known mineralized zones as well as detection of new ones. The surveys were initially undertaken with an axial probe and multiple transmitter loops in July 1991, however from November, 1991 the then recently released three component probe system was used.

System Settings

Data for all surveys were collected with the following settings:

Transmitter Loop Size:	200m x 200m
Loop Current:	10 Amps
Base Frequency:	25 Hz (10ms off-time)
Ramp:	1 msec
Time Windows:	17 channels, with the first centered at 0.09 msec after the ramp and the last, at 5.9 msecs (see Figure 1).
Units:	$nT/s=nV/m^2$
Axial Probe Equiv. Area:	$6500m^2$
XY Probe Equiv. Area:	$2800m^2$

Drill-hole SH20

During routine axial probe DHEM surveying of drillhole SH20, from 5 transmitter loops in a "+" shaped configuration (Figure 6), two off-hole conductors were detected. Intermediate to late-time data (using these terms in a relative sense) for each loop are shown in Figure 7. The primary field patterns for the eastern, central and western loops are shown in Figure 8.

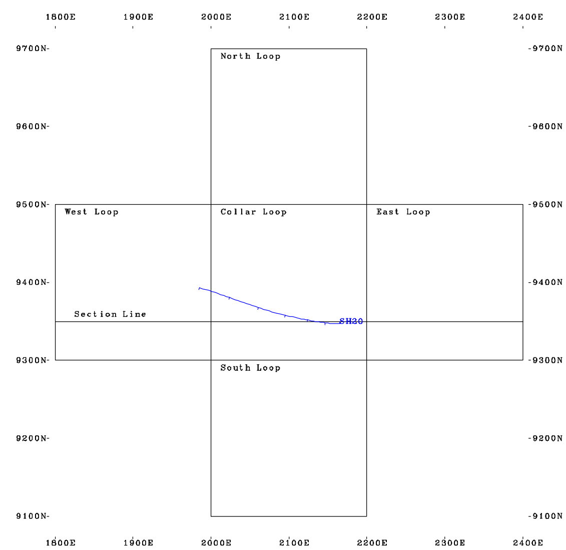

Figure 6. Configuration of the five transmitter loops used for the axial probe DHEM surveys of drill-hole SH20.

Analysis of Multiple-Loop Axial Data

Two separate responses can be seen in each of the profiles in Figure 7. The shallower one, at ~75m, corresponds with known Zone 1 mineralization, however the off-hole response recorded at 225m was unexpected. There was no evidence for its cause in the core, but it correlates with Zone 4 mineralization, which had been intersected more than 100m south of SH20.

Because of the vertical depth at which the deeper conductor lies and its narrow width, there is some ambiguity as to whether the conductor is located above or below (east or west of) the hole, and its lateral extent. Drill-hole data in long section tends to favour an up-dip location.

A comparison of amplitudes of the north, collar and south loop data indicates that the bulk of the deeper (conductive) and east loops implies a conductor located closer to the central and west loops, with the west loop suggesting a conductor above the hole. The shape of the anomaly is distorted by the response from the shallower conductor which adds ambiguity to dip interpretation, but the reverse coupling between east and west loops (Figure 8) suggest a dip of ~40° to 50° to the (south) east.

Because the mineralization has a high aspect ratio geometry, the shape and orientation of induced current patterns will be dictated by the intermediate conductor width. As a result modelling with a simple filament can result in a conductor being fitted to the data, that is either north or south, above or below the drill-hole for most loops.

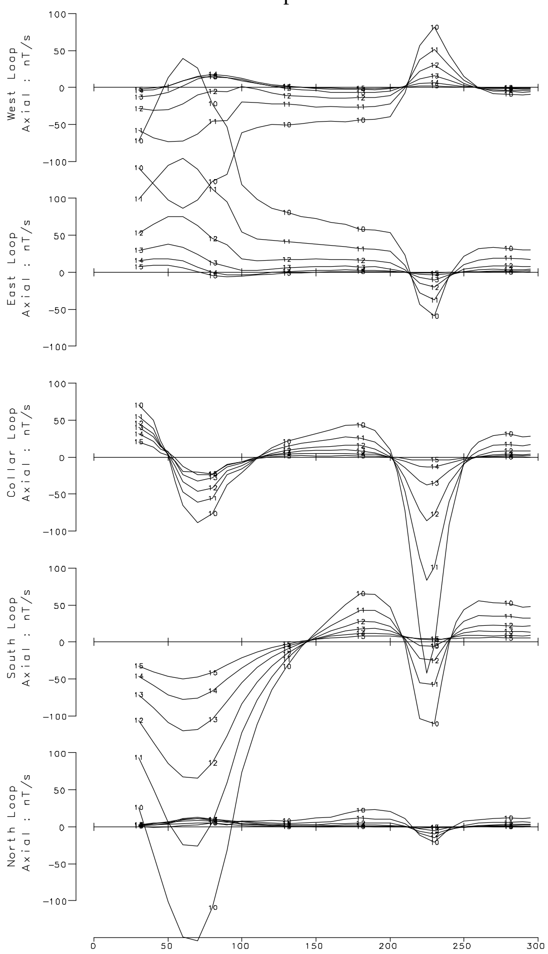

Figure 7. Intermediate to late time (~1 to 3.5 msec) axial DHEM data for SH20 for the five loops shown in Figure 6. The shallow response at ~75m is due to known Zone 1mineralisation. The response at ~225m was unexpected, but correlates to Zone 4 mineralisation intersected ~ 100m to the south.

Three component data

Cross-component data was recorded using only the central loop (Figure 9). Unlike the results from axial data, the three-component results are unambiguous. The deeper conductor is definitely above, and mainly to the south of, the drill-hole. (Figure 10 shows the X and Y data before and after rotation, as well as displaying the amount of probe rotation from the local UA plane).

Modelling of the data using the programme "Filament" (Duncan, 1995) for an east dipping, NNE trending conductor, above and to the south of the drill-hole, gives a very good fit in the mid-time channels (Figure 11).

Figure 12 shows the axial response from the collar loop in linear-logarithmic format as well as displaying comparisons of the Raw, Cleaned and Calculated PP. There is very little difference between the measured, calculated and cleaned PP in this instance.

Drill-hole SHL940

Drill-hole SHL940 lies to the north of SH20 and was surveyed with both axial and cross-component probes from two transmitter loops, north and south. Since the southern transmit loop corresponds most closely with the collar transmit loop for SH20 (Figure 13) only this data is used for comparison of results.

Figure 14 presents the three sets of data, U, V and A, for SHL940 from the south loop. As a check, the hole was logged twice with the cross-component probe and the rotated (i.e., corrected) data from the two runs agree closely.
Drill pipe in the top 70 m of the hole excluded this region from being surveyed and results in an inconclusive model data fit to the shallower Zone 1 mineralization. The deeper conductor is reasonably well resolved with regard to local cross-overs and minima and maxima, however there is significant side-lobe distortion due to zone 1. Nevertheless, simple filament modelling of the data gives a good fit to Zone 4 (not shown), with the final model similar to that generated from the SH20 collar loop data.

Integrated Interpretation

Both the multi-loop axial data and the single loop three component data for SH20 suggest that Zone 4 does not extend north of SH20, either as a continuous lens or as discrete lenses and this is supported by the data collected in SHL940.

Hole BRCD111 (Figure 13) was drilled to the south of SH20 to follow up the zone 4 mineralization, which was intersected at a depth of approximately 200 m in the hole.

Because of the high aspect ratio for the mineralized lenses, and shallow dip, it is expected that direct current techniques such as applied potential would assist in mapping the extent of the lenses.

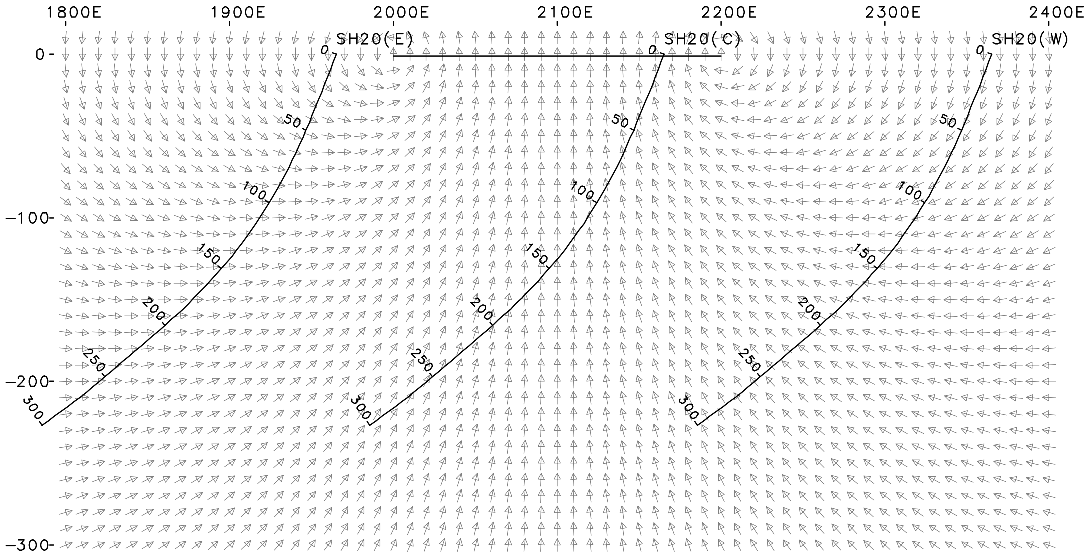

Figure 8. Primary field directions for section 9350N for the West, East and Collar loops showing the opposing coupling directions for the eastern and western loops in the target zone at ~225m down the hole.

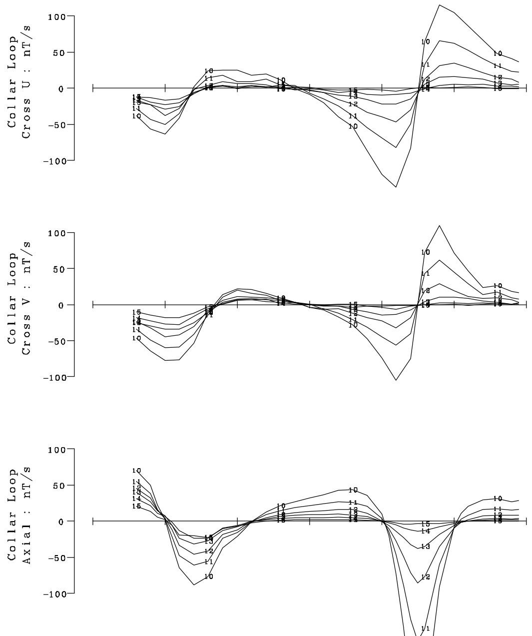

Figure 9. Intermediate to late time (~1 to 3.5 msec) three component DHEM data for the collar loop for drill-hole SH20. Clear responses in each component for the deeper (Zone 4) conductor allow a more confident interpretation of conductor location and orientation.

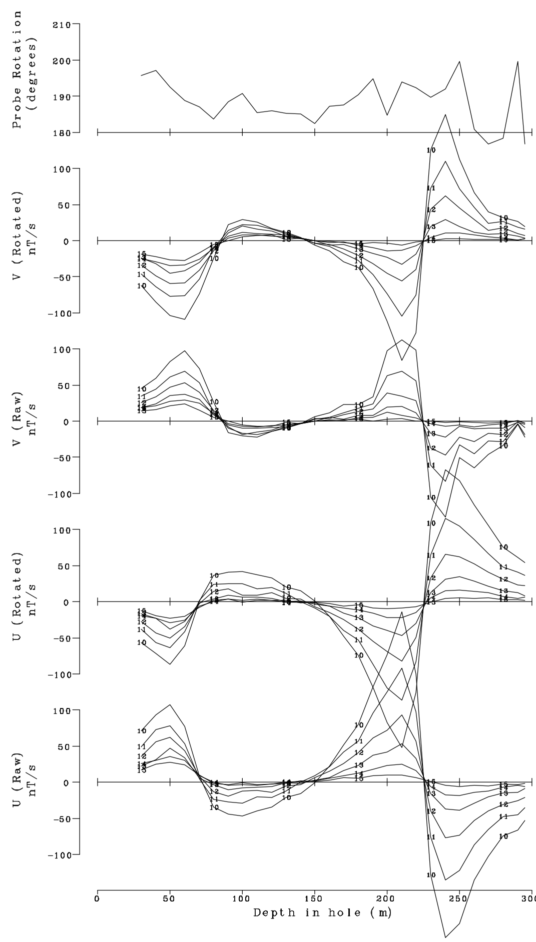

Figure 10. Raw and rotated UV data and amount of rotation, for collar loop for drill-hole SH20. Rotation of more than 180 deg. produce sign changes in the 'U' and 'V' component data.

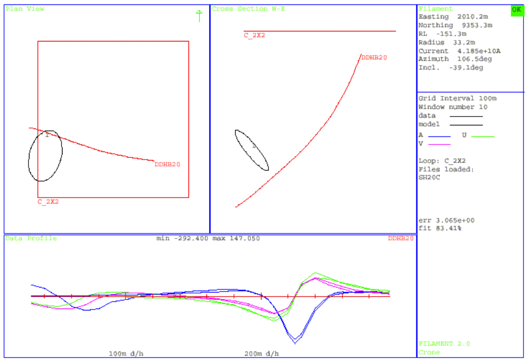

Figure 11. Filament model results for mid-time channel (0.95 msec) for 3 component data collected in drill-hole SH20 using the collar loop. A close fit to the observed data is obtained from an east dipping, NNE trending conductor lying above, and to the south of, SH20.

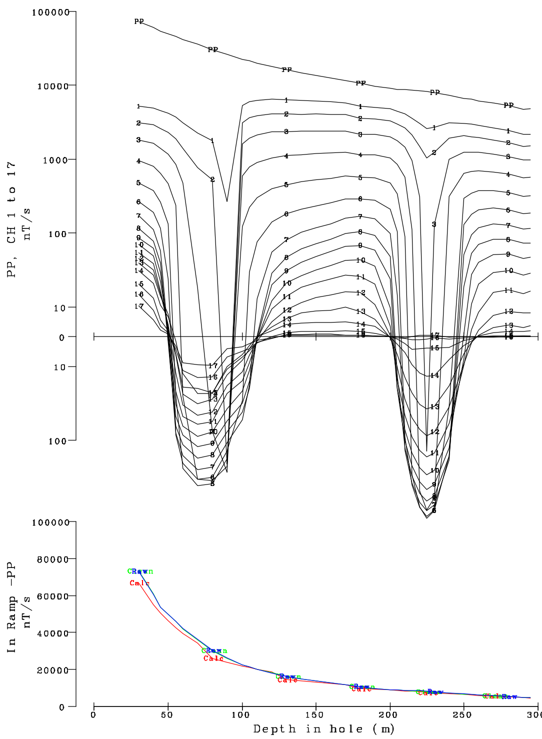

Figure 12. (a) Semi-logarithmic plot of the SH20 collar loop axial data and (b) linear profiles of the Raw, Cleaned, and Theoretical PP response. In this particular example the conductors adjacent to the hole have not noticeably distorted the primary pulse and thus the ‘cleaning’ has made little difference to the observed (Raw) PP

Vector Presentation of Data

A vector presentation of multi-component data can be an effective way to present the data and may assist in initial interpretation. Figure 15a shows the directions (as arrows) and amplitudes (as profiles) of the XY data for window 10 (~0.95 msecs) in a plan projection of the two holes, and Figure 15b, the XZ data in cross-section view for the holes.

This data presentation method helps overcome the problems of dynamic range in plotting profiles and assists in the initial interpretation, when trying to “visualize” the response in the drill-hole(s), of a particular transmitter loop/conductor combination.

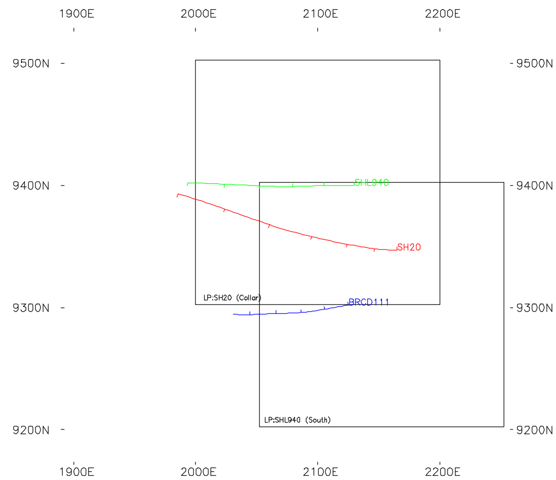

Figure 13. Plan map showing location of drill-holes SH20 and SHL940, and their respective loops, and the follow up drill-hole BRCD111.

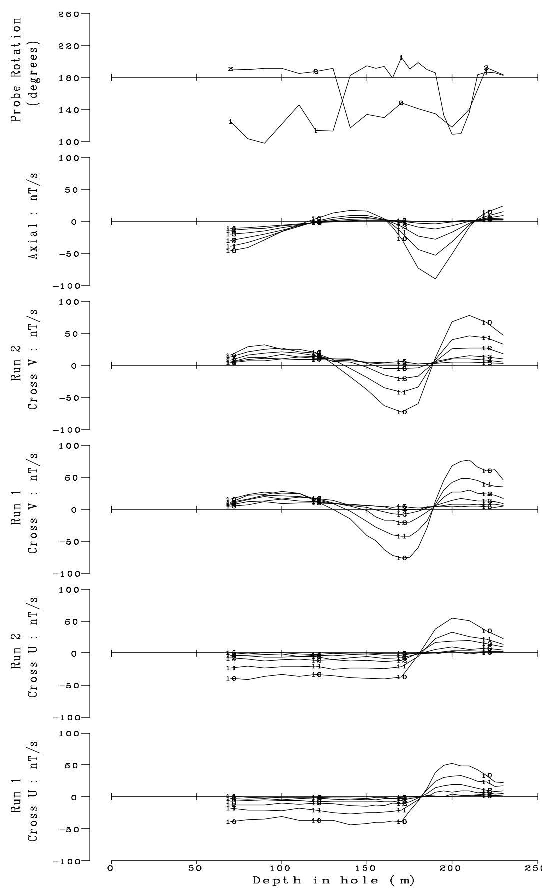

Figure 14. Comparison of two sets of corrected UV data from drill-hole SHL940 using the southern transmitter loop. The figure shows that the procedure to correct for probe rotation using the PP is capable of producing very repeatable results.

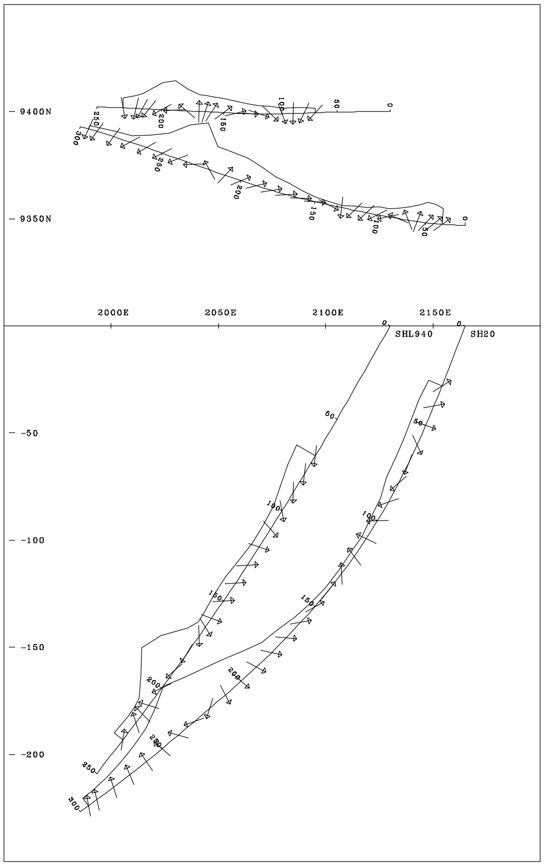

Figure 15. Vector data presentation for SH20 (collar loop) and SHL940 (south loop) for channel 10 (0.95 msec). The figure shows the direction (arrows) and amplitude (profiles) of (a) the XY data in plan projection and (b) the XZ data in cross section. The data are compatible with a source lying to the south of, an above SH20.

CONCLUSION

DHEM surveying at the Balcooma VMS deposit located a previously unknown extension of a lens of mineralization. Axial data, and later, three component data were collected, with a much more confident interpretation obtained from the latter. Multiple loops are still required to ensure maximum coupling to potential conductors as well as aiding discrimination between conductors.

Examples of multi-component data showed that clean, repeatable data could be obtained using the primary field, “cleaned” from the influence of adjacent (including target) conductors, to correct the probe’s rotation.

Finally, presentation of multi-component DHEM data in vector form, in a similar manner to that used in three component drill-hole magnetometry, is shown to be a concise and useful way to present results.

ACKNOWLEDGMENTS

The authors would like to thank Lachlan Resources and Pasminco Ltd for permission to publish the data in this paper. We would also like to thank S. Moore for supplying the geological cross-section and M. Green and P. Basford for their many useful comments. Finally we would like to acknowledge both John Bishop and James Macnae for their comments and contributions whilst reviewing this paper.

REFERENCES

Asten, M.W., 1987, Full transmitter waveform transient electromagnetic modeling and inversion for soundings over coal measures: Geophysics, 52, 279-288.

Barnett, C.T., 1984, Simple inversion of time-domain electromagnetic data: Geophysics, 49, 925-933.

Cull, J.P., 1993, Downhole three component TEM probes. Exploration Geophysics (1993) 24, 437-442.

Duncan, A.C., 1987, Interpretation of down-hole transient EM data using current filaments. Exploration Geophysics 18, 36-39.

Dyck, A.V., 1987, Drill-hole electromagnetic methods in Nabighian, M.N., Ed., Electromagnetic methods in applied geophysics, Soc. Expl. Geopys,. Vol 1, 881-930.

Harvey, K.J., 1984, The discovery of the Balcooma massive sulphides deposit, in Geoscience in the Development of Natural Resources, Seventh Australian Geological Convention, Sydney, Geol. Soc. Austr. Abstr., 12:218-219.

Hodges, D.G. and Crone, J.D., 1991, A new multiple component downhole pulse EM probe for directional interpretation, in Proceedings of the 4th International MGLS/KEGS Symposium on Borehole Geophysics for Minerals, Geotechnical and Groundwater Applications; Toronto, 18-22 August 1991.

Huston, D.L and Taylor, T.W., 1990, Dry River copper and lead-zinc-copper deposits, in Geology of the Mineral Deposits of Australia and Papua New Guinea (Ed. F.E Hughes), pp. 1519-1526.

Lachlan Resources NL. 1992, 1995. Annual Report

Ravenhurst, W., 1992, Case History Note, Crone History Note, Crone Geophysics & Exploration Ltd.

APPENDIX: PRIMARY PULSE CLEANING

The direction of the primary field can be used to determine the orientation of a cross-component DHEM probe which has undergone an arbitrary rotation in the drill-hole. However, in the presence of a conductor, the field may become distorted and unusable. This appendix describes a method of recovering the primary field value.

Assume that the idealized current in a transmitter loop is a 50% duty cycle square waveform with a peak current of “I” amps, and where the shut off occurs via a controlled ramp with shut-off time of “R” seconds as shown in Figure A1. Then in free space, the induced voltage in a perfect coil would be as shown in Figure A2, where the amplitude G can be positive or negative and is a constant geometrical factor which accounts for the coil position with respect to the loop and component of the field being measured.

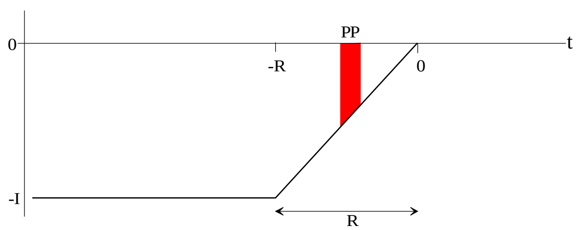

Figure A1. Input current waveform with a shut off ramp of width R.

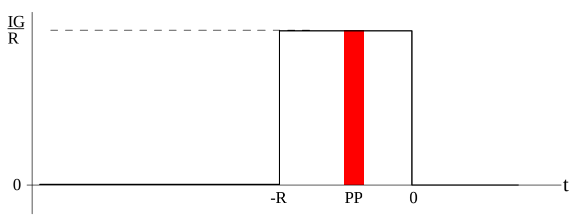

Figure A2. The induced voltage in a perfect coil in free space for the transmitter waveform shown in Figure A1 (I – loop current, G – geometric factor, R – ramp width).

Due to secondary induced fields, this square pulse is distorted. Figure A3 shows the addition of secondary fields of various strengths and polarity from poor and good conductors for a particular component.

We require the free space value IG/R (PP) in order to relate it to the calculated values. Figure A3 shows that for poor conductors, the measured PP will be close to that for free space, but for good conductors which decay more slowly, we need to “clean” the PP measurement to arrive at the free space values.

In order to determine the distortion in the PP channel, it is convenient to consider the impulse response of the earth H(t). This is the response observed when the current in the transmit loop consists of a unit step. If this function is known, then the measured response is just the convolution of the actual rate of change of the current waveform with the impulse response of the earth (Asten, 1987).

If we consider for the moment only the current ramp, our measured response will be:

$$A(t)=H(t)*C(t)$$

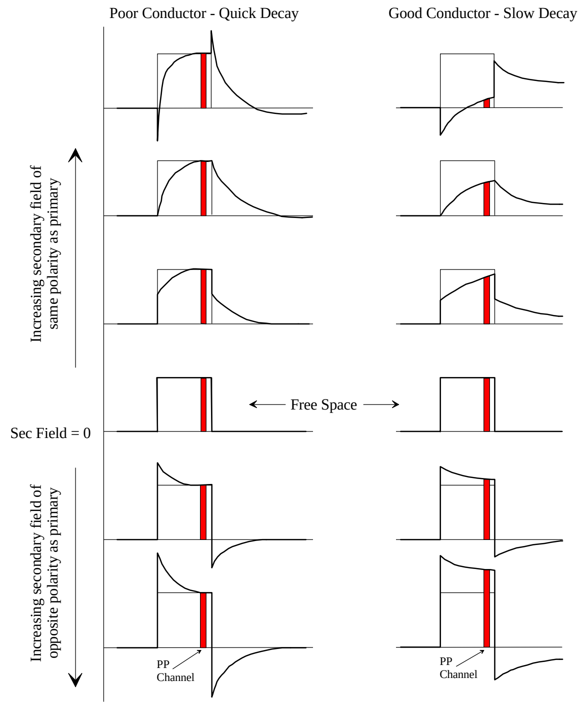

Figure A3. Examples of distortion in the primary field (PP) due to induced secondary fields from poor and good conductors.

Where

A(t) is the measured response
H(t) is the earth’s impulse response
C(t) is a square pulse of amplitude 1/R
And * is the convolution operator.

This is equivalent to:

$$A(t) = \tfrac{I}{R} \int_{t}^{t+R} H(t')dt' \qquad (1)$$

If we introduce a scaled impulse response:

$F(t) = \frac{H(t)}{G}$, where G is as defined previously**,**

Then F(t) represents the response from a current step in the transmitter loop of I/G and well have an area under the curve that is always unity:

$$\int_{0}^{\infty} F(t)dt = 1$$

Substituting in (1), we get:

$$A(t) = \tfrac{IG}{R} \int_{t}^{t+R} F(t')dt' \qquad (2)$$

For the case of channels within the ramp (-R<t<0), we use the fact that F(t) = 0 for t < 0 to get:

$$A(t) = \tfrac{IG}{R} \int_0^{t+R} F(t')dt' ; \text{ -R < t < 0}$$

If we set t = P, the Crone Primary Pulse channel time, we get:

$$PP = A(P) = \tfrac{IG}{R} \int_0^{P+R} F(t')dt' ; \text{ -R < P < 0}$$

Thus, it can be seen that the measured PP is equal to the theoretical value IG/R only when the integral is unity. This will occur only if the integral covers the entire impulse response (i.e. the response has decayed to zero by time P+R), which correlates to a poor conductor with a quick decay. The measured response at time P+R is given by:

$$A(P+R) = \tfrac{IG}{R} \int_{P+R}^{P+2R} F(t')dt'$$

And the response at P+2R is given by:

$$A(P+2R) = \tfrac{IG}{R} \int_{P+2R}^{P+3R} F(t')dt'$$

These values generally represent samples in the off-time at times R and 2R from the PP channel position. Summing this progression to infinity would give:

A(P) + A(P+R) + A(P+2R) +…

$$= \tfrac{IG}{R} \int_0^{P+R} F(t')dt' + \tfrac{IG}{R} \int_{P+R}^{P+2R} F(t')dt' + \tfrac{IG}{R} \int_{P+2R}^{P+3R} F(t')dt' + ...$$

$$= \tfrac{IG}{R} \int_0^{\infty} F(t')dt'$$

$$= \tfrac{IG}{R}$$

which is the required free space value.

In practice, providing that an appropriate repetition rate is used, the function F(t) has normally decayed to zero by the end of the off-time, so that the summation can stop there with sufficient accuracy. (Assuming an exponential decay, it can be shown that if the sampling time, w, of the transmitting waveform (i.e., the off-time), is expressed in terms of the time constant, τ, of a primary-field-distorting conductor, then if $w=10\tau$, we get close to 100% of the correct value, but this is reduced to ~65% if $w=\tau$, and down to ~10% for $w=0.1\tau$. For examples shown in this paper, conductors with time constants of up to ~4 milliseconds would not significantly affect the measured primary pulse.)

Taking as an example, the case of small secondary field in the same direction as the primary inducing field, we can look at the response as being the difference between two identical IG/R step responses offset in time as shown in Figure A4.

Thus by taking the PP reading and adding samples spaced a distance R apart, starting from the PP position, we get the value of the step response at the point of the last sample in the summation. If we continue the summation to the end of the off-time, we will have the free space PP value, provided the transient from a single IG/R step response has decayed to zero within that time.

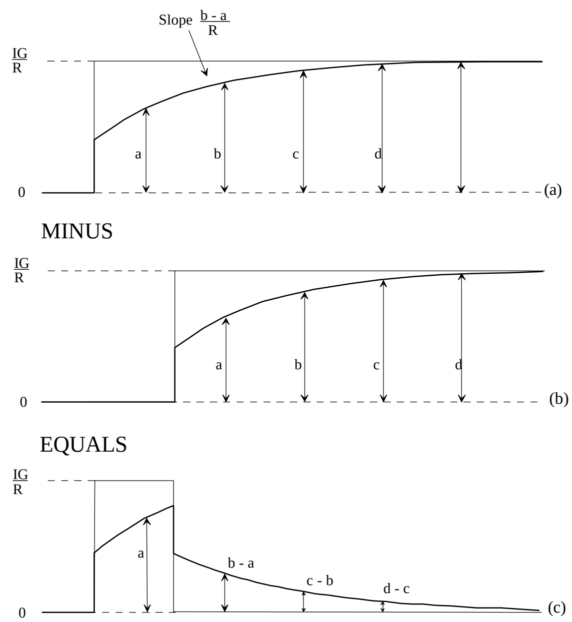

Figure A4. The received waveform can be regarded as the difference between two identical step responses separated by time R.

A field example of cleaning PP distortion from NW Tasmania

To illustrate the application of PP cleaning, we present an example from north-west Tasmania. The hole, HP03, has been drilled through a thick sequence of conductive shales (the Que River Shales). Figure A5(a) shows the recorded results, which indicates a broad, in-hole response, plus the observed PP. Data was collected using the Crone 10 channel option and a 10 msec off time resulting in 8 channels of off-time data being recorded, plus PP. Figure A5(b) shows the raw PP (which is the same as the observed PP), the cleaned PP and the theoretical PP. Even though the off-time is not sufficient to fully resolve the decay (Figure A6) this has only a minor effect on the calculation of the cleaned PP. (The discrepancy between the cleaned PP and the theoretical PP near the top of the hole is attributed to an inexact knowledge of the loop location with respect to the drill-hole).

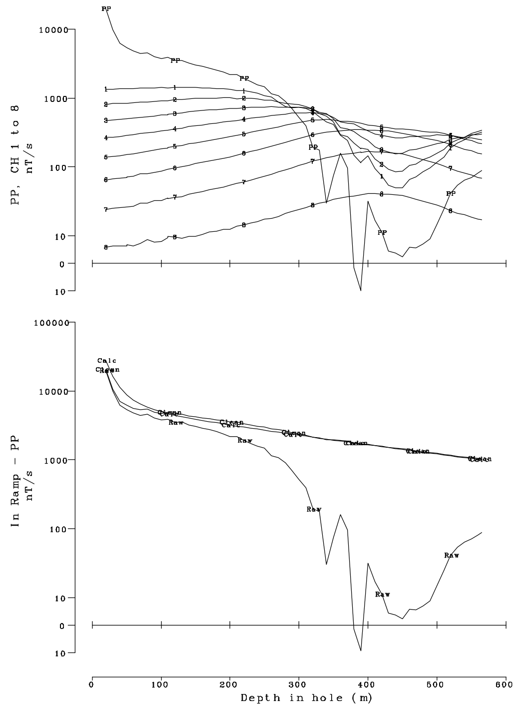

Figure A5. (a) Measured secondary field for DDH HP03 showing a broad in-hole response. The recorded PP shows considerable distortion. (b) The Raw, Cleaned and Theoretical PP. The cleaning process has removed much of the distortion allowing the PP to be used for cross-component probe rotation. (The discrepancy between the theoretical and cleaned PP near the top of the hole, is attributed to positional inaccuracies between the loop and drill-hole.)

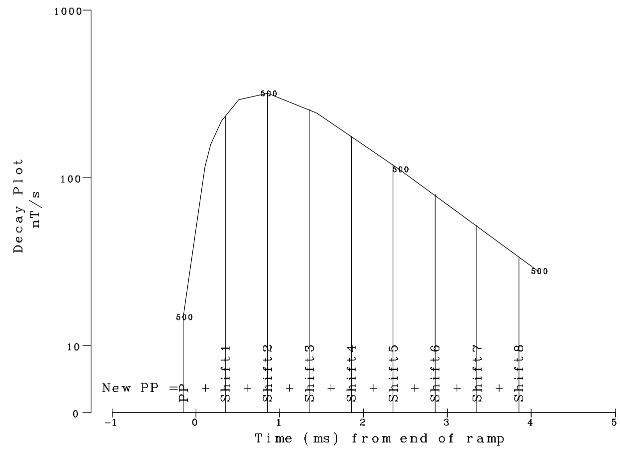

Figure A6. The observed decay at 500m down DDH HP03. This shows the observed (raw) PP and the numerous additions read off the decay curve (in steps of ‘R’) to form the final cleaned PP. Using the 10 channel option and 10 msec off time results in the collection of 8 channels of data plus the PP channel.